Growth and production of the brittle stars *Ophiura sarsii* and *Ophiocten sericeum* (Echinodermata: Ophiuroidea)

Alexandra M. Ravelo[*1], Brenda Konar[1], Bodil Bluhm[2], Katrin Iken[1]

[*](907) 474-7074

amravelo@alaska.edu

[1]School of Fisheries and Ocean Sciences, University of Alaska Fairbanks

P.O. Box 757220, Fairbanks, AK 99775, USA

[2]Department of Arctic and Marine Biology, University of Tromsø

9037 Tromsø, Norway

Abstract

Dense brittle star assemblages dominate vast areas of the Arctic marine shelves, making them key components of Arctic ecosystem. This study is the first to determine the population dynamics of the dominant shelf brittle star species, *Ophiura sarsii* and *Ophiocten sericeum*, through age determination, individual production and total turnover rate (P:B). In the summer of 2013, *O. sarsii* were collected in the northeastern Chukchi Sea (depth 35 to 65 m), while *O. sericeum* were collected in the central Beaufort Sea (depth 37 to 200 m). Maximum age was higher for *O. sarsii* than for *O. sericeum* (27 and 20 years, respectively); however, both species live longer than temperate region congeners. Growth curves for both species had similar initial fast growth, with an inflection period followed by a second phase of fast growth. Predation avoidance in addition to changes in the allocation of energy may be the mechanisms responsible for the observed age dependent growth rates. Individual production was higher for *O. sarsii* than for *O. sericeum* by nearly an order of magnitude throughout the size spectra. The distinct distribution pattern of the two species in the Alaskan Arctic may be determined by environmental characteristics such as system productivity. Both species had equally low turnover rates (0.2 and 0.1, respectively), similar to Antarctic species, but lower than temperate species. Such characteristics suggest that the dense brittle star assemblages that characterize the Arctic shelf system could have a recovery time from disturbance on the order of decades.

Key words: population dynamics; brittle stars; age; growth; production; turnover rate; Arctic

Introduction

The longevity and growth pattern of the inhabitants of a region can provide information regarding the carrying capacity, biological interactions and stability of the marine system they inhabit (Carroll et al. 2011a, Dolbeth et al. 2012). Environmental influence on growth is especially important in porlar regions, where the effects of low temperatures and the seasonality of food supply are reflected in the slower growth rate and often-larger body size of polar benthic invertebrates compared with lower latitude taxa (Brey & Clarke 1993, Bluhm et al. 1998, Sejr et al. 2002, Blicher et al. 2007). The ongoing climate-associated changes on Pacific Arctic shelves that are particularly relevant to Arctic benthic organisms include the increase in water temperature and changes in water column primary production (Woodgate et al. 2010, Arrigo & van Dijken 2015). These changes may affect the metabolic rate, growth and production of benthic organisms, which in turn can alter benthic production and energy transfer to higher trophic levels. Currently, our sparse knowledge of the population parameters for Arctic benthic species, particularly brittle stars, limits our ability to model the energy flow through the Alaskan Arctic benthos adequately, and from making solid projections for future climate scenarios (Hoover 2013, Whitehouse et al. 2014).

This study took place in the Alaskan Arctic, which encompasses two distinct shelf systems in the Chukchi and Beaufort Seas. The Chukchi Sea has an inflow shelf that receives nutrient rich waters originated in the Pacific and Bering Sea. These water masses support high seasonal primary production on the Chukchi shelf, which in conjunction with low zooplankton grazing translates into high deposition of organic matter to the benthos (Grebmeier et al. 2006, 2015). In contrast, the Alaskan Beaufort Sea has a narrow interior shelf highly influenced by upwelling and riverine input (Jakobsson et al. 2012). Along the slope from the west, inflowing modified Pacific water enters the Beaufort Sea through Barrow Canyon (Carmack & Macdonald 2002, Nikolopoulos et al. 2009). The high benthic biomass on the Chukchi Sea shelf thereby extends into the western Beaufort Sea outer shelf and slope, supported by the inflow of highly productive waters (Logerwell et al. 2011, Ravelo et al. 2014). On the Canadian Beaufort Shelf, with the exception of periods of upwelling, low water column primary production is mostly limited by nutrients and light availability (Carmack et al. 2004). Along with *in situ* and advected components of marine production, the Beaufort shelf receives abundant terrestrial carbon related to riveriene inflow and coastal errosion (Goñi et al. 2013).

The two dominant Arctic shelf brittle star species are *Ophiura sarsii* and *Ophiocten sericeum* (Frost & Lowry 1983, Bluhm et al. 2009, Ravelo et al. 2014, Ravelo et al. 2015). These species have a wide distribution, similar life cycle (broadcast spawners with planktonic larvae) and are predator-scavengers occupying similar trophic levels (Tyler 1977, Piepenburg 2000, Fetzer & Deubel 2006, Iken et al. 2010, Divine et al. 2015). The large bodied *O. sarsii*, with a maximum disc diameter of 40 mm, is a circumpolar species found as far south in the Pacific as 35° N (Piepenburg 2000). Throughout the Chukchi Sea shelf and western Beaufort Sea slope, *O. sarsii* outnumbers all other brittle star species, and locally all other epibenthic taxa, accounting for up to 71% of the average epibenthic abundance of 34 ind. m^{-2} (Ravelo et al. 2014). In the highly productive northeast Chukchi Sea, with an average biomass estimate for epibenthos of 62.7 g wet wt. m^{-2}, brittle stars (mainly *O. sarsii*) accounted for 39% of that biomass (Ravelo et al. 2014). The smaller-bodied *O. sericeum*, with a maximum disc diameter of 18 mm, is a circumpolar species found in various habitats north of 40° N (Piepenburg 2000). *Ophiocten sericeum* is especially abundant in interior shelves, such as the central Beaufort shelf and Laptev Sea (Piepenburg et al. 1997, Roy et al. 2015, Ravelo et al. 2015). On the central Beaufort Sea shelf, the average abundance of epibenthic invertebrates per station was four ind. m^{-2}, with *O. sericeum* accounting for nearly 40% of the total abundance of that region (Ravelo et al. 2015). In general, brittle stars are important prey for crab and demersal fish; however, relatively low predator abundance and generally small fish size may be factors contributing to the high density of brittle stars in many Arctic regions (Tyler 1972, Aronson 1989, Packer et al. 1994, Rand & Logerwell 2010, Divine et al. 2015). In terms of carbon remineralization brittle star assemblages can be responsible for 25-40% of the total benthic respiration on Arctic shelves (Ambrose et al. 2001, Renaud et al. 2007). Despite the wide distribution of these brittle star species, their local dominance over all other epibenthic taxa, and their ecological importance in energy transfer through the marine system, little is known of their individual growth and production, as well as the temporal stability of these assemblages (Piepenburg 2000, 2005).

This study determined the growth and production of the Alaskan Arctic shelf dominant brittle star species, *O. sarsii* and *O. sericeum* through age, population size structure, individual production and total turnover rate. Given the similarities of the two species in terms of their circumpolar distribution and biological traits, we hypothesized that 1) the growth curves of *O. sarsii* and *O. sericeum* have similar shapes, showing an initial period of fast growth that decreases gradually with increasing body size until achieving asymptotic size, similar to other brittle star species. Because *O. sarsii* dominates in the highly productive Chukchi Sea region and is absent on the less productive central Beaufort shelf, it is possible that the less productive region is not capable of sustaining a larger species with a higher energetic demand, such as *O. sarsii*. Therefore, the high densities of *O. sarsii* may not only be a function of the highly productive system in which it dominates, but also a product of high individual production values. With this in mind, we formulated the following hypotheses, 2) *O. sarsii* has higher individual production values compared with individuals of *O. sericeum* of the same size, and 3) *O. sarsii* has a higher turnover rate (P:B ratio) than *O. sericeum*.

Methods

Sample collection

In both the Chukchi and Beaufort seas, brittle stars were collected using a 3.05 m plumb-staff beam trawl (PSBT) with a 7 mm mesh and a 4 mm codend liner (Gunderson & Ellis 1986); however, a modified version (PSBT-A) was used on very soft sediment stations in the Beaufort Sea (Abookire & Rose 2005). The trawl time ranged from 1 to 5 minutes on the seafloor at a vessel speed of 1 to 1.5 knots, the distance trawled ranged from 63 m to 383 m. *Ophiura sarsii* were collected at 20 stations in the NE Chukchi Sea at water depths ranging from 35 to 65 m during the August 2013 COMIDA-CAB Hanna Shoal cruise (Chukchi Sea Monitoring In Drilling Area-Chemical And Benthos). Sampling sites in the Chukchi Sea were selected by random generation using a hexagonal tessellation approach to ensure sites were randomly, yet evenly distributed through the Hanna Shoal study area (Fig. 1; Ravelo et al. 2014). *Ophiocten sericeum* were collected in the central Beaufort Sea during the August 2013 US-Canada Transboundary cruise at 17 stations, with water depths ranging from 37 to 200 m (Bell et al. 2016). Sampling sites in the Beaufort Sea were in part chosen to repeat previously sampled locations by other research projects and additional sampling stations were selected at a spacing approximately 0.5° latitude and 0.25° longitude with the goal to cover the majority of the along-shelf extent of the central Beaufort Shelf (Fig. 1).

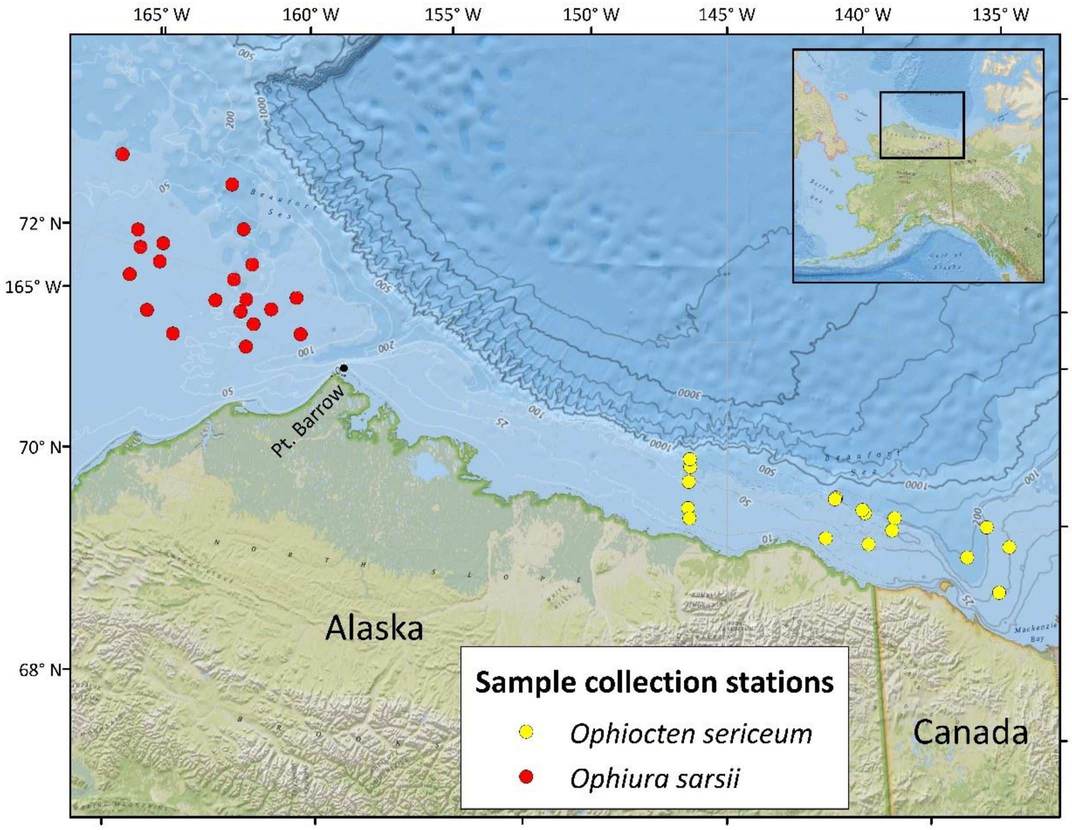

Fig. 1. Collection sites for brittle stars, July-August 2013. Specimens of *Ophiura sarsii* were collected in the northeastern Chukchi Sea, and specimens of *Ophiocten sericeum* were collected in the central Beaufort Sea

Age, size frequency and organic mass determination

At each station, all brittle stars were counted and a total weight recorded. For *O. sarsii,* 115 to 350 individuals were haphazardly selected from each station and disc diameters were measured. These measured individuals were then frozen and later processed at the University of Alaska Fairbanks (UAF). For *O. sericeum,* 95 to 380 individuals were collected from each station, immediately frozen and later processed at UAF. For both species, disc diameter was measured from the base of one arm to the opposite interradius (Hyman 1955), with an accuracy of 0.1 mm using digital calipers. Individuals that were too small or fragile for handling were measured from a digital image using ImageJ software(Abramoff et al. 2004). For this purpose, individuals were placed on a flat contrasting surface, with a ruler for size calibration, and photographed using a digital camera. The mode of the population sampled was determined with the MODE function in Excel. Subsamples of the brittle stars used for size frequency distributions that showed no evidence of damage or regenerated arms were used for aging and organic mass (OM) content analysis. To ensure an even representation of all sizes, 10-12 individuals were haphazardly selected for every 1 mm body size increment. Individuals at the extremes of the size spectrum (largest and smallest) were collected outside of the size frequency samples to increase the size range for aging and OM samples.

The determination of growth and age was performed through the measurement and quantification of annual growth bands in the skeletal structure of the arm ossicles (Gage 1990a). Each arm ossicle is composed of a central articulating condyle and four surrounding fossae. The skeletal structure of the ossicle is composed of a three-dimensional meshwork called stereom. Changes in the microstructure of the stereo, from high density to low density, can be seen in a band pattern throughout the fossae (Fig 2). These changes in density correspond to seasonal variations in growth; therefore, the combination of two seasonal changes in stereom density would represent one year of growth. Because the band patterns are consistent throughout the fossae, total age can be determined (Gage 1990b, Wilding & Gage 1995, Dahm & Brey 1998, Gage 2003). Evidence from other ophiuroid age studies indicates that as individuals grow, the stereom of the central part of the ossicle develops over the fossa, concealing the early growth bands of the larger individuals and, therefore, an age correction is necessary (Dahm & Brey 1998). Age correction was, therefore, applied following the back-calculation method described in Dahm and Brey (1998). Through this method, the first band of the smallest sized individuals, those with clearly no overgrown bands because the size of the visible band is greater than the concealing area, determined the size of the first growth band or age 1 (VB1max). With increasing body size, if the measurement of the first visible band exceded VB1max, then the band was defined as VB2max and one year was added to the total age. Successively, with increasing individual body size and depending on the size of the first visible growth band (exceeding VB2max, VB3max or VB4max, etc.), more growth bands were added to the total count (2, 3 or 4, etc.) (Fig. 2a).

The ossicles used for aging came from the base of four arms of each individual sampled (the fifth arm and disc were used for OM determination). Tissue was removed by soaking each arm in 5% sodium hypochlorite at 60 °C for 10 to 60 minutes (depending on the size of the arm) and later washed with distilled water. For each individual, a single ossicle was mounted on a stub and coated with gold for microstructure examination using a scanning electron microscope (SEM) at the Advanced Instrumentation Laboratory, UAF (Gage 1990a, 1990b). Ossicle growth measurements (using ossicle radius, R) were taken along a transect of the upper right or left fossa, determined by a 45° angle from the vertical axis that runs through the center of the ossicle (Fig. 2a). Growth bands were measured along the same longitudinal axis from the center of the ossicle to where the stereom changed from fine pores to large pores (Fig. 2b). All measurements were performed directly on each SEM image using ImageJ. Accuracy of growth band measurement and count were assessed three times by the same person. First, growth bands were marked on all images. In a second round, growth bands marked were reassessed for accuracy and measured. Finally, a third quality control assessment was performed for each image and measurements before all measurement values were compiled.

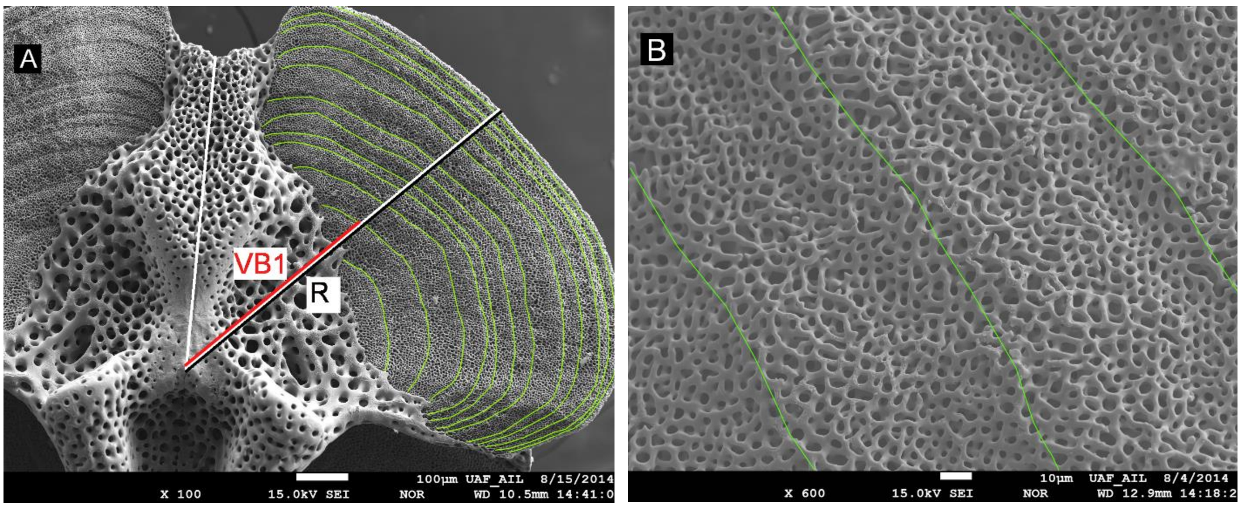

Fig. 2. Scanning electron microscope image. (a) *Ophiura sarsii* ossicle with the 45° angle (white line) illustrating the longitudinal axis used to measure ossicle radius and count growth bands. Ossicle radius R (black line) was used to define the linear relation between ossicle and body size. All visible growth bands are highlighted and illustrate the intercept with measurement axis. Measurement of the first visible growth band that intercepts with measurement axis is labeled VB1 (red line). (b) Magnified view of growth bands showing transition between fine pore stereom and large pore stereom on the fossae

Two growth models were applied to the corrected size-at-age data using the Virtual Handbook to Population Dynamics, which uses the iterative Fit by Excel-Solver based on the NEWTON nonlinear fitting algorithm (Brey 2001). The models used were the Special von Bertalanffy growth function

(1) $$DD_t = DD_\infty\left(1 - e^{-K(t-t_0)}\right)$$

and the Gompertz growth function:

(2) $$DD_t = DD_\infty e^{-e^{-K(t-t^*)}}$$

where DD_t is the size at age t (in mm disc diameter), DD_∞ is the asymptotic size (in mm), K is a growth constant per year, and t_o is the age at size zero (in years), while t^* is the age at the inflection point of the curve (in years).

Because of the difficulty of obtaining brittle stars with all arms intact, only one complete arm was used for OM content analysis in addition to the central disc. The single complete arm and the disc were processed separately to obtain the OM weight. Total arm organic mass was calculated by multiplying by five the weight of the single arm processed. Disc and the single arm of each specimen were dried in an oven at 60° C for a minimum of 24 hours, after which they were incinerated for 10-12 hours in a muffle furnace at 500° C. All weights were recorded with a precision of 10 μg on a microscale. Organic mass value for each specimen was calculated as ash-free dry mass as follows:

(3) $$OM=[DDW+(5ADW)]-[DAW+(5AAW)]$$

where DDW and ADW are the disc and single arm dry weight, respectively. DAW and AAW are the disc and arm ash weight, respectively.

The mass specific growth rate, $MSGR$ (y^{-1}), was calculated using the size-mass relationship and the parameters of the von Bertalanffy growth function:

(4) $$MSGR=bK(DD_\infty - DDi)/DDi$$

where K is the growth parameter of the von Bertalanffy growth function, DD_∞ is the maximum or asymptotic size, DDi is the mean-diameter of size class i (determined by the best fitted growth model for each species), and b is the slope of the size mass relationship.

The organic mass production for each size class (i), Pi (g AFDM y^{-1} m^{-2}), was calculated as:

(5) $$P_i=MSGR_iOM_iN_i$$

where OMi and Ni are the mean individual organic mass and the number of individuals in size class i standardized to m^2, respectively. The total annual production is:

(6) $$P=\sum Pi$$

The total P:B (y^{-1}) ratio was calculated from total production across all size classes (P, g AFDM y^{-1} m^{-2}) and the average biomass (g AFDM m^{-2}) of all stations. Because biomass in the field was measured in wet weight, a conversion factor was applied from the individual wet weight to organic mass, using the same subsample of the population used to determine individual OM. For *O. sarsii*, the conversion factor was 0.120421 g OM per g wet weight (N = 260), while for *O. sericeum* the conversion was 0.143318 g OM per g wet weight (N = 137).

Results

Age and growth

Out of the 256 *O. sarsii* ossicle samples imaged, 150 were clear enough to measure and quantify growth bands. Of the remaining 106 samples not included in the age analysis, 72% had unclear growth bands, 11% had anomalous calcium carbonate growth covering parts of the fossae, and 17% had other issues (i.e., edge of the fossa was damaged or the fossa edge was tilted back). From the 147 *O. sericeum* samples imaged, 98 were clear enough to measure and quantify growth bands. Of the remaining 49 samples, 64% had unclear growth bands, 30% had anomalous calcium carbonate growth covering at least parts of the fossae, and 6% had other issues (as above). Outliers for both species were excluded for having markedly higher or lower numbers of growth bands in comparison with individuals of similar disc diameter (see Appendix, Fig. 9 a-d). For *O. sarsii*, eight samples, ranging from 14 to 19 mm DD, were excluded from growth parameter calculations as outliers, reducing the total sample size to 142 samples. For *O. sericeum*, four samples, ranging from 2 to 13 mm DD, were excluded from growth parameter calculations as outliers, reducing the total sample size to 94 samples.

Corrected ages in *O. sarsii* ranged from 1 to 27 years. Age correction for *O. sarsii* resulted in the addition of up to nine years to the number of visible growth bands of the largest individuals (Fig. 3a and 3c). The corrected ages of *O. sericeum* ranged from 2 to 20 years. Visible age band readings were adjusted by adding up to six years in the largest individuals (Fig. 3b and 3d).

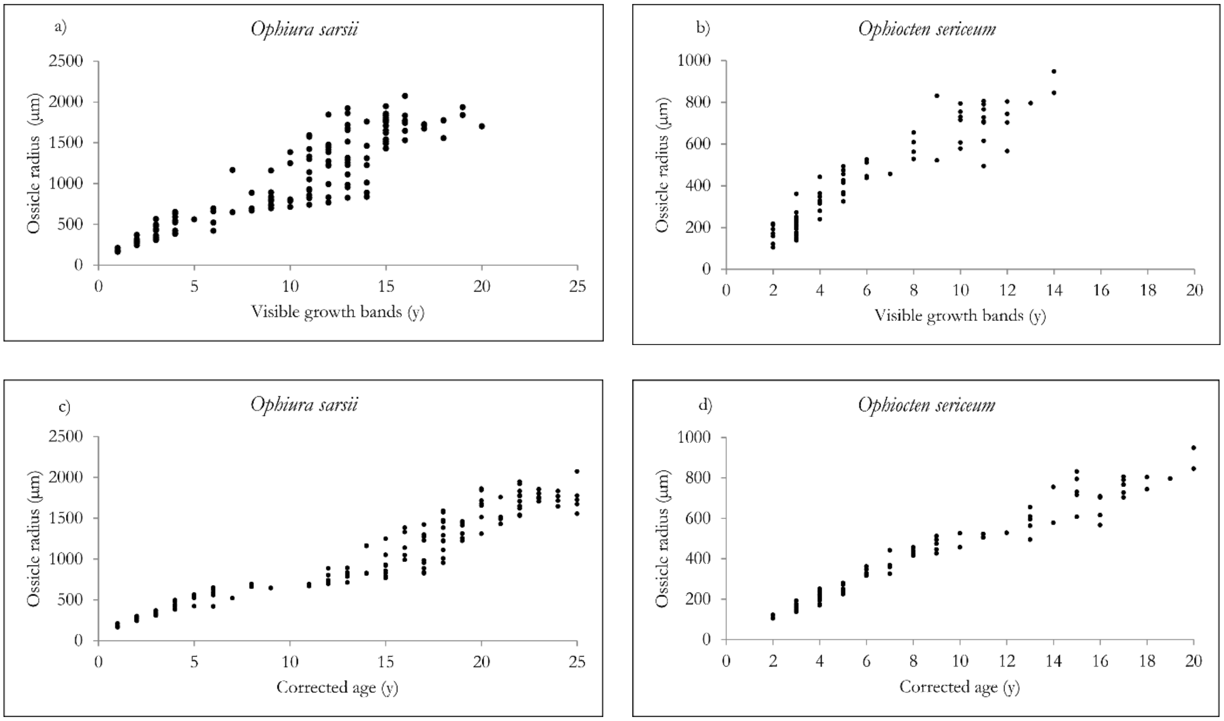

Fig. 3. Ossicle radius (µm) as a function of the visible growth band of *Ophiura sarsii* (a) and *Ophiocten sericeum* (b). Body size (measured in disc diameter, mm) as a function of the corrected age of *O. sarsii* (c) and O. sericeum (d). For *O. sarsii* N =142 and for *O. sericeum* N =94

Body size-at-age determination was possible given the significant linear relation between body size and ossicle radius for both species ($p < 0.05$). For *O. sarsii*, increase in body size explained 98% of the increase in ossicle radius (Fig. 4a). For *O. sericeum*, the increase in body size explained 97% of the increase in ossicle radius (Fig. 4b).

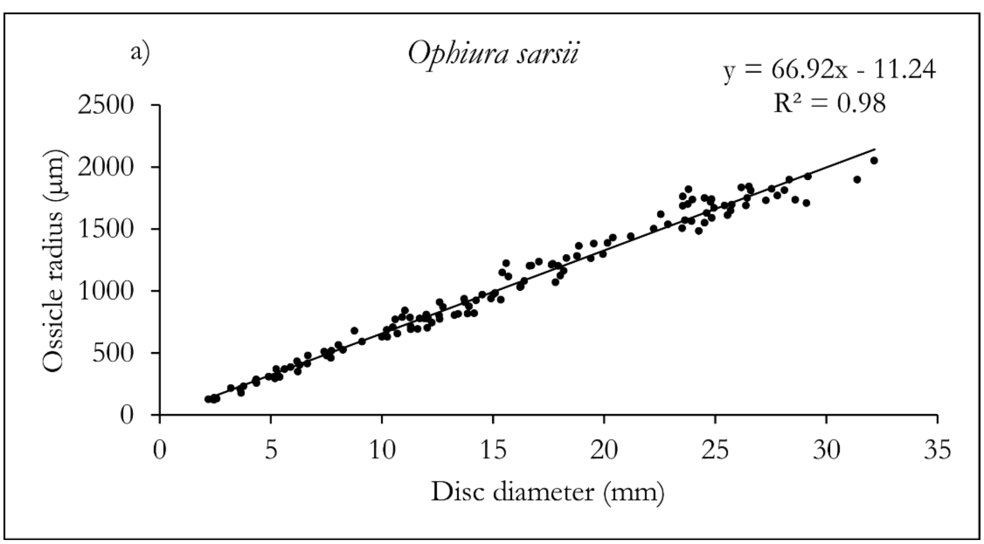

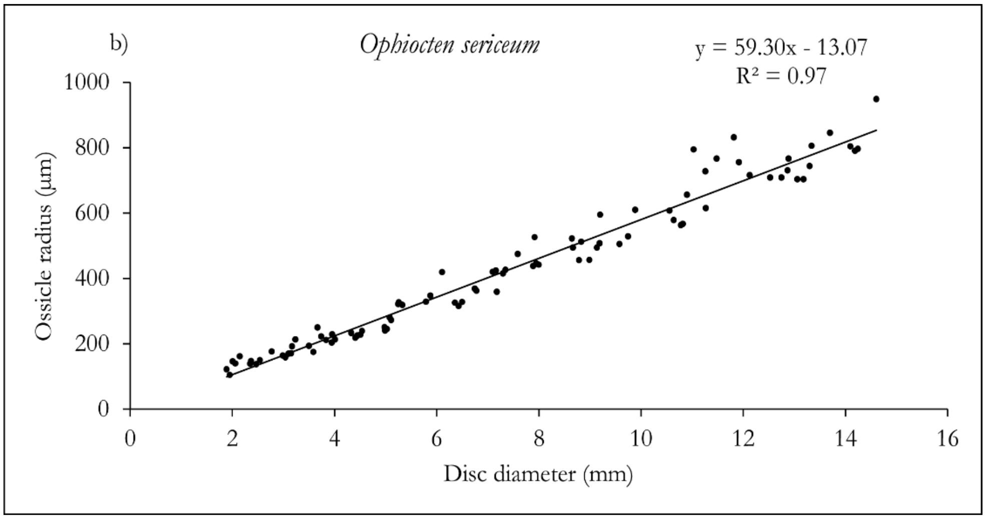

Fig. 4. Linear relation between the ossicle radius and body size (disc diameter, mm) for (a) *Ophiura sarsii* (N = 150) and (b) *Ophiocten sericeum* (N = 98)

The two growth models (Gompertz and specialized von Bertalanffy) had very high and similar R^2 for both species (Fig. 5). However, for *O. sarsii* the Gompertz model resulted in the lower residual sum of squares, while for *O. sericeum,* the best fit resulted from the von Bertalanffy model (Table 1). According to the best fit model for each species, the asymptotic size was 40 mm for *O. sarsii* and 20 mm *O. sericeum* (Table 1, Fig. 5). The growth rates computed with the best fit model for each species were very similar (*O. sarsii*, $K = 0.077$ and *O. sericeum* $K = 0.065$). The age at size 0 (von Bertalanffy model) was very similar for both species (*O. sarsii*, $to = 0.65$ and *O. sericeum*, $to = 0.50$), while the age of inflection point of the Gompertz model was greater for *O. sarsii* ($t^* = 14$ years) than for *O. sericeum* ($t^* = 10$ years) (Table 1).

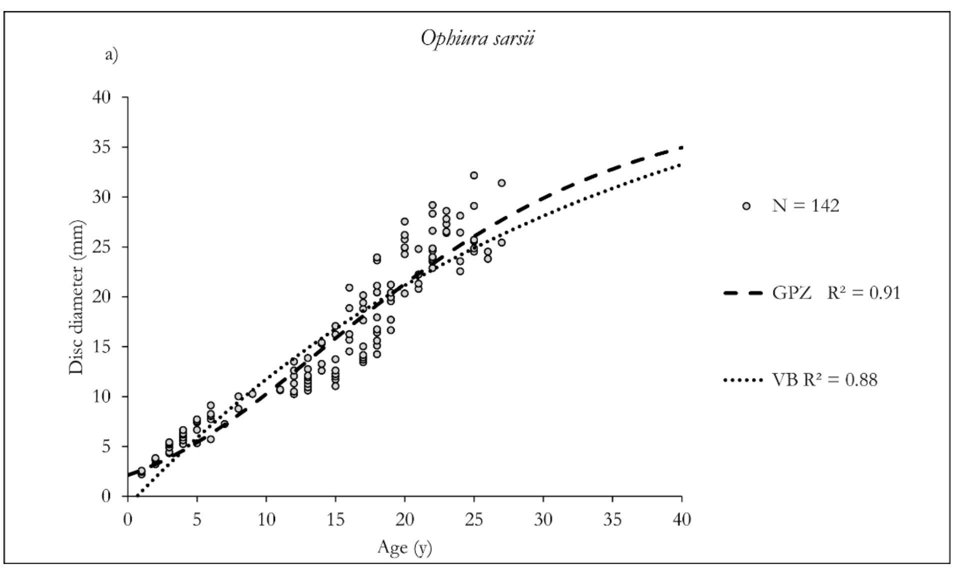

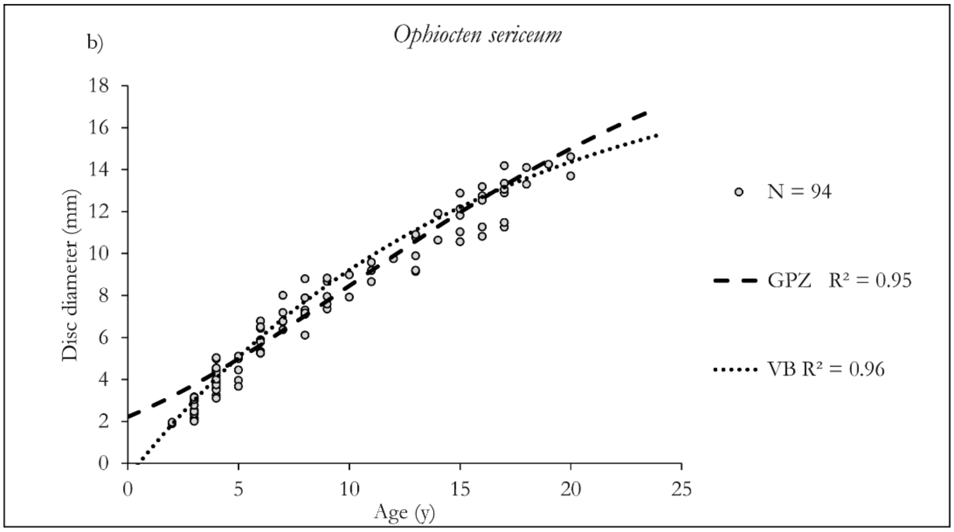

Fig. 5. Fitted growth curves for body size (disc diameter, mm) as a function of corrected size at age data for (a) *Ophiura sarsii* and (b) *Ophiocten sericeum*. Gompertz growth curve (GPZ) marked with dashed line and von Bertalanffy growth curve (VB) marked with dotted line

Table 1. Growth models for *O. sarsii* and *O. sericeum*. Parameters for each model are, *DD*∞ is the asymptotic size (mm disc diameter), *K* the growth rate per year, *t** the inflection point of the Gompertz curve and *to* the age at size 0 (years) of the von Bertalanffy model. The goodness of fit for each model is expressed in R^2 and RSS (residual sum of squares = Sum(S-S')²) values

	Model	DD∞	K	t* or t_o	R^2	RSS
Ophiura sarsii	Gompertz	40	0.077	14.00	0.91	817.99
	von Bertalanffy	48	0.030	0.65	0.88	1099.53
Ophiocten sericeum	Gompertz	23	0.085	10.00	0.95	69.44
	von Bertalanffy	20	0.065	0.50	0.96	57.63

Individual production and turn-over rates

Body size of *O. sarsii* ranged from 1.8 to 30.9 mm and the mode of the population was 8.2 mm (N = 6,478) (Fig. 6a). For *O. sericeum,* body size ranged from 1.1 to 14.9 mm disc diameter and the mode of the population was 2.9 mm (N = 3,683) (Fig. 6b).

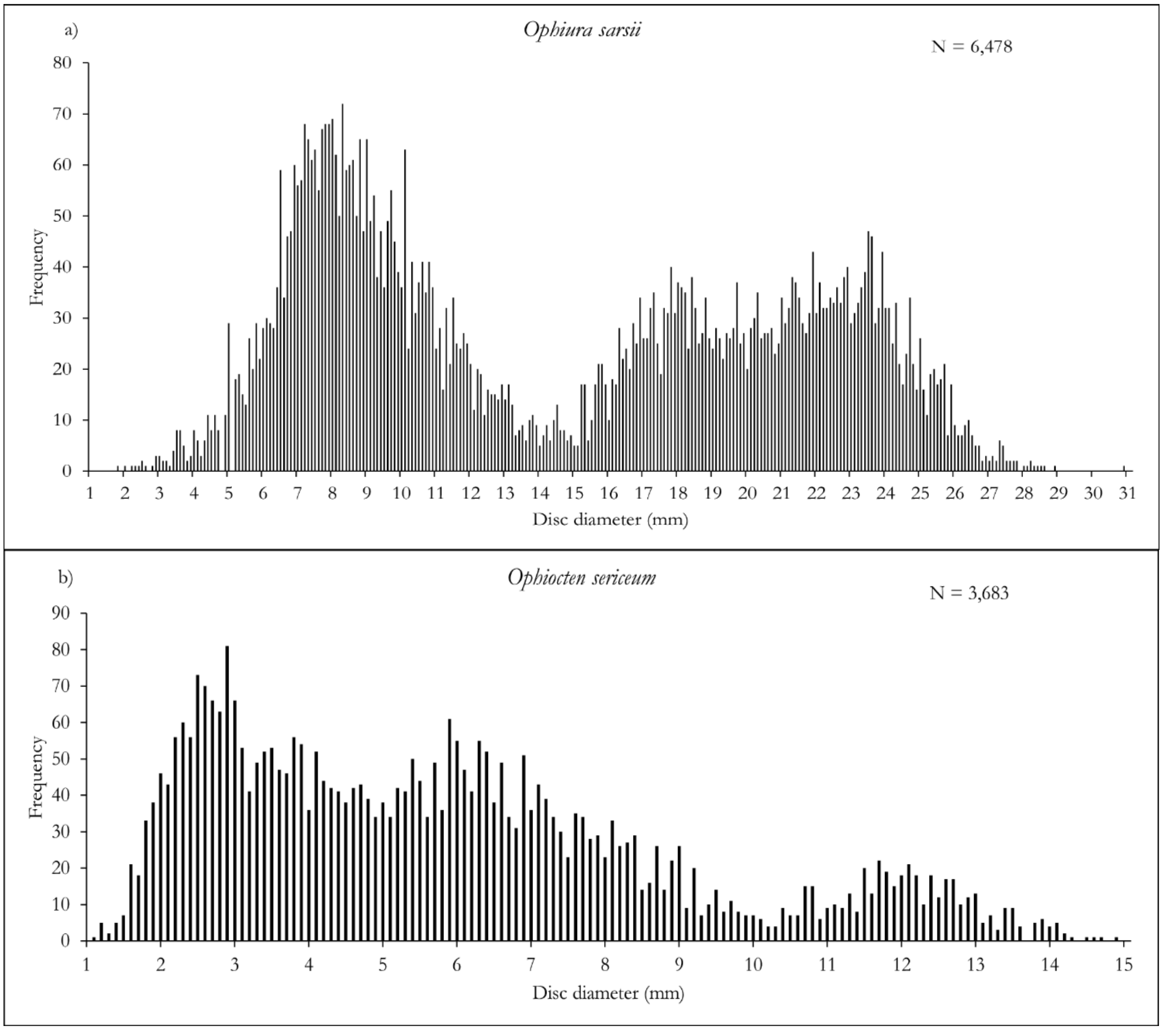

Fig. 6. Absolute size frequency distribution for a representative subsample of the population of (a) *Ophiura sarsii* collected in the NE Chukchi Sea (N = 6,478) and (b) *Ophiocten sericeum* (N = 3,683) collected in the central Beaufort Sea

A total of 260 *O. sarsii* individuals were used for organic mass determination, ranging from 2.4 to 32.2 mm disc diameter. The following equation determined the organic mass to body size relationship with an $R^2 = 0.95$ (Fig. 7a).

$$OM=2\times10^{-4}DD^{2.3953} \quad (7)$$

For *O. sericeum*, a total of 137 individuals were used for organic mass determination, ranging from 1.9 to 14.6 mm disc diameter. The following equation determined the organic mass to body size relationship with an $R^2 = 0.97$ (Fig. 7b).

$$OM=8\times10^{-6}DD^{3.4564} \quad (8)$$

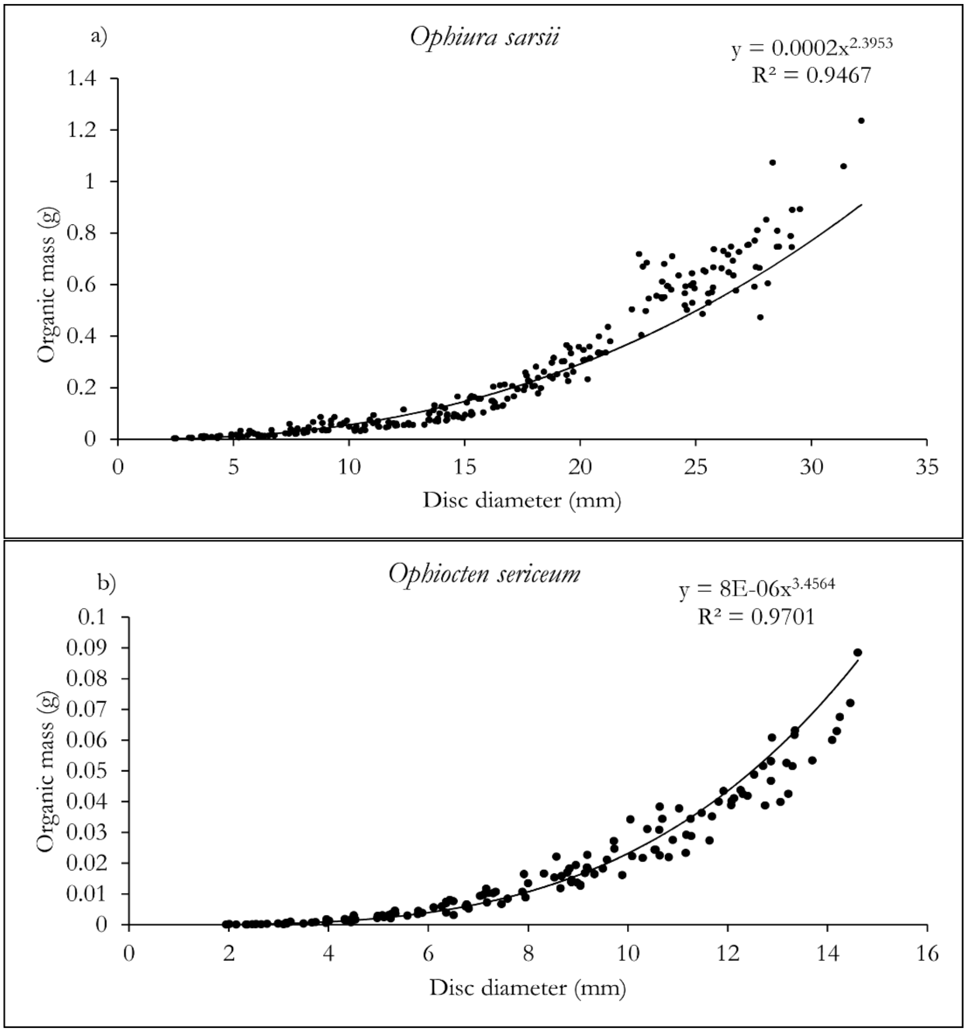

Fig. 7. Organic mass content as a function of body size (disc diameter, mm) for (a) *Ophiura sarsii* (N =260) and (b) *Ophiocten sericeum* (N = 137). Ash free dry mass (AFDM) in g

The average station biomass for *O. sarsii* was 5.69 g wet wt. m^{-2} (sd: 4.41, range: 0.48 - 16.55) or 0.69 g OM m^{-2} after conversion (N = 20 stations). The average abundance per station in the study region was 392 ind. 100 m^{-2} (sd: 451, range: 22 - 1,543). From the mass specific growth rate (MSGR), the total annual organic mass production and the production to biomass ratio (P:B) amounted to 0.13 g y^{-1} m^{-2} and 0.20 y^{-1}, respectively (Table 2). Individual production increased with body size until it peaked at size class 23.3 mm and later remained constant at slightly lower values until the largest size class recorded (Fig. 8a).

For *O. sericeum,* the average station biomass was 0.96 g wet wt. m^{-2} (sd: 1.35, range: 0.06 - 3.78) or 0.1413 g OM m^{-2} (N = 14 stations). The average abundance per station in the study region was 680 ind. 100 m^{-2}, (sd: 1066, range: 11 - 4,030). From the MSGR, the total P and P:B amounted to 0.02 g y^{-}

^{1} m^{-2} and 0.11 y^{-1}, respectively (Table 2). Individual production increased steadily with body size, until size class 10.2 mm where it remained relatively constant until the last size class recorded (Fig. 8b).

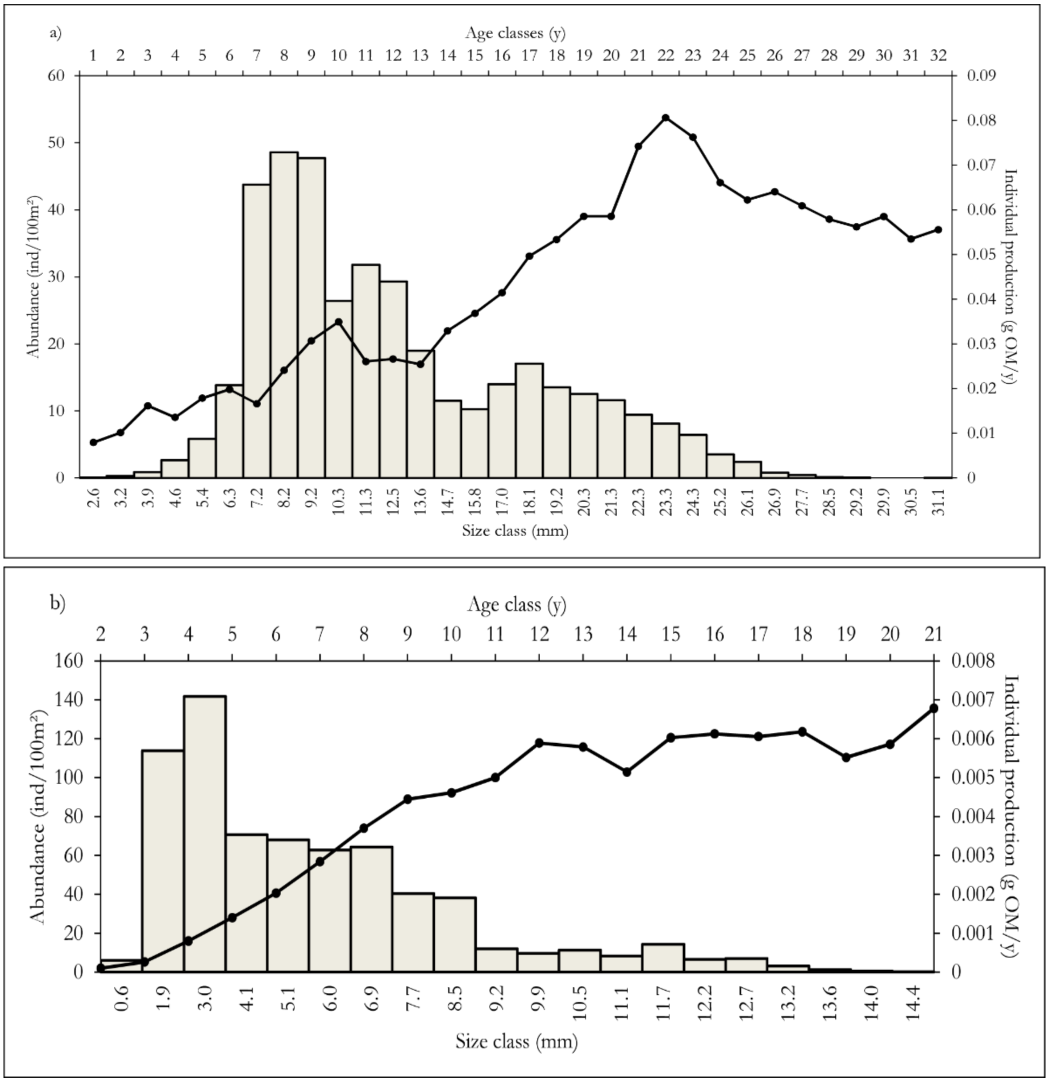

Fig. 8. Distribution of size and age classes for the standardized abundance of the sampled population (bars, ind/100m2) and individual production (line, g AFDM/y) for (a) *Ophiura sarsii* and (a) *Ophiocten sericeum*. Size and age classes were defined by the best fitted growth models for each species. Size as disc diameter in mm and age in years (y)

Table 2. Published values for production, biomass and turnover rate of other brittle star species along with values from this study, updated from Dahm (1996) (Table 5-26). All weights are AFDM (ash free dry mass), where P is the annual production (g m^{-2} y^{-1}), B is the average biomass (g m^{-2}), P:B is the turnover rate (y^{-1}) and mean body mass (mg of AFDW). (*) indicate averages of values published for several study sites.

Region	Species	Study region	Mean body mass	P	B	P:B	Source
Arctic	*Ophiura sarsii*	Chukchi Sea	30.00	0.13	0.69	0.20	this study
	Ophiocten sericeum	Beaufort Sea	3.00	0.02	0.14	0.11	this study
Antarctica	*Astrotoma agassizii*	Weddell and Lazarev Seas*	690.00	0.02*	0.28*	0.05*	Dahm (1996)
	Ophioceres incipiens	Weddell and Lazarev Seas*	20.00	0.11*	0.52*	0.20*	Dahm (1996)
	Ophionotus victoriae	Weddell and Lazarev Seas*	210.00	0.07*	0.39*	0.19*	Dahm (1996)
	Ophiurolepis brevirima	Weddell and Lazarev Seas*	90.00	0.05*	0.37*	0.14*	Dahm (1996)
	Ophiurolepis gelida	Weddell and Lazarev Seas*	30.00	0.30*	0.20*	0.14*	Dahm (1996)
Temperate to Sub-Arctic	*Amphiura chiajei*	North Atlantic - Irland	177.47	49.62	139.32	0.36	Munday and Keegan (1992)
	Amphiura filiformis	North Atlantic - Irland	30.00	31.50	21.00	1.50	O'Connor et al. (1986)
	Amphiura filiformis	Sweden - Gullmarsfjord	21.00	2.59	5.63	0.42	Skold et al. (1994)
	Ophiocten gracilis	North Atlantic - Rockall Trough	0.75	X	X	0.73	Gage and Tyler (1982a)
	Ophiocten gracilis	North Atlantic - Rockall Trough	X	0.26*	0.30*	0.86*	Gage (2003)
	Ophiomusium lymani	North Atlantic - Rockall Trough	1010.14	X	X	0.33	Gage and Brey (1994)
	Ophiothrix fragilis	North Atlantic - Bristol	42.80	31.43	17.30	1.82	George and Warwick (1985)
	Ophiura albida	North Sea	5.13	0.35	1.12	0.32	Dahm (1993)

	Ophiura ljungmani	North Atlantic - Rockall Trough	1.96	X	X	0.54	Gage and Tyler (1981)
	Ophiura ljungmani	North Atlantic - Rockall Trough	0.25	X	X	1.26	Gage and Brey (1994)
	Ophiura ophiura	North Sea	2.85	0.53	1.21	0.43	Dahm (1993)
	Ophiura ophiura	North Atlantic - Bristol	79.06	0.55	0.81	0.68	Warwick et al. (1978)
	Ophiura ophiura	North Atlantic - Bristol	7.87	0.11	0.24	0.50	Warwick and George (1980)
Sub-Antarctic	*Ophionotus hexactis*	South Georgia	48.75	3.39	7.45	0.45	Morison (1979)
Tropical	*Amphioplus coniortodes*	Atlantic - Florida	21.04	2.41	1.07	2.26	Singletary (1971)
Tropical	*Micropholis gracillima*	Atlantic - Florida	23.15	2.90	1.30	2.23	Singletary (1971)
Tropical	*Ophionephtys limicola*	Atlantic - Florida	70.82	5.60	2.41	2.33	Singletary (1971)

Discussion

Age and growth

The validation of the annual periodicity of growth bands, though lacking for ophiuroids, has been determined for other high latitude echinoderms. For ophiuroids, the seasonal change in the density of the stereom was previously demonstrated with the temperate species, *Ophiura ophiura* (Wilding & Gage 1995). Similarly, in the present study the vast majority of ossicles of *O. sarsii* and *O. sericeum* had the edge of the fossae formed by large pores (low density stereom), corresponding to the high productive season when they were collected (Arrigo et al. 2014). Techniques such as mark-recapture or tank experiments using tetracycline or calcine staining, used to validate growth mark increments of fish, mollusks, sea urchins and other fauna, could be considered in future research focused on brittle stars.

Based on the growth patterns of other brittle star species, we hypothesized that *O. sarsii* and *O. sericeum* would have similarly shaped growth curves, characterized by initial fast growth that decreases gradually with increasing body size, until achieving asymptotic size at similar maximum ages. This hypothesis was supported in that both species had indeed similarly shaped growth patterns; however, the predicted size at age pattern was not supported. Rather, growth of *O. sarsii* and *O. sericeum* followed an apparent oscillatory pattern, with an initial period of fast growth (for approximately eight years in both species), followed by a ceasing in growth (four to five years), resulting in an inflexion in the growth curve and, finally, a second period of accelerated growth with no clearly reached asymptotic age. Despite the high correlation values of the growth models applied, the predicted growth did not conform well to the distribution of size by age; as a result, growth was simultaneously over and under-estimated by the model outputs (Fig. 5).

As observed for many invertebrates, the growth pattern of both brittle star species could be a result of a combination of development strategies and predation pressure (Clarke 1980, Brey 1991). The allocation of energy to fast growth in early life stages allows the smaller brittle stars to escape high predation pressure (Gage 1990b). For example, significantly higher predation was reported for the smaller sizes of *O. sarsii* (3-13 mm DD) by the flatfish American plaice (*Hippoglossoides platessoides*) in the north Atlantic, even when larger size classes were available (Packer et al. 1994). As prey of fish and crab, larger brittle stars must allocate energy to arm regeneration due to cropping during non-fatal attacks; however, smaller brittle stars may be consumed entirely (O'Connor et al. 1986, Packer et al. 1994, Sköld & Rosenberg 1996, Divine et al. 2015). For Arctic brittle stars, allocating energy exclusively to growth early in life should prove advantageous considering the increased predation pressure on smaller body sizes.

Reproductive processes, such as the onset of gonadal development and spawning, require energetic expenses that result in reduced energy allocation to somatic growth in adult marine invertebrates (Brey 1991, Storero et al. 2010, Stevenson & Mitchell 2016). Alongside, the high seasonality of food supply and low temperatures, characteristic of polar environments, may require polar species to allocate energy selectively to growth or reproduction throughout their life (Clarke 1980, Brey 1991). Gametogenic analysis of the deep-sea brittle star *Ophiomusium lymani* showed that developed gonads were only present in individuals larger than the mid-size classes (Gage & Tyler 1982). While ophiuroids present many developmental strategies (i.e. planktotrophic and direct development), for species with planktonic larvae, the number and size of the ova are directly related to the size of the individual (Hendler 1975). Therefore, allocating most energy to gonad production after a certain body size would optimize the reproductive outcome, which is especially important in regions, such as the Arctic shelves, with extreme seasonality in food supply. The inflection period in the growth curves, may be a life stage in which gonad development and activation may prevail resulting in slow somatic growth for these brittle star species. With increasing size, adult brittle stars may be able to allocate energy to both reproduction and growth, as seen in the second phase of the growth curves for both species.

Increased longevity and slow growth are characteristic of many polar invertebrate species, including echinoderms (Brey & Clarke 1993, Ambrose et al. 2006, Gusev & Jurgens-Markina 2012). Our results, in addition to being the first records of age for Arctic brittle stars, concur with the trend of higher maximum ages of polar *versus* subpolar, temperate and tropical species (Dahm 1993, Gage 2003, Sköld et al. 2001). Maximum age for the two sub-Arctic congeners of *O. sarsii*, *Ophiura albida* and *Ophiura ophiura* was equaly nine years (Dahm 1993), which is considerably lower than the maximum age of 27 years determined for *O. sarsii*. Compared with the maximum age of 20 years determined for *O. sericeum*, the sub-Arctic *Ophiocten gracilis* had a considerably lower maximum age of seven years (Gage 2003). Recent analysis of growth rates along a latitudinal gradient showed a strong linear relationship between echinoid growth rates and temperature, with polar species growth falling significantly below the projected linear trend (Peck 2016). The high seasonality of food availability in polar regions has also been discussed as a major contributor to the reduced growth rate of benthic invertebrates inhabiting these regions (Brey & Clarke 1993, Blicher et al. 2007). Though the mechanisms for the increased longevity of polar organisms is not entirely clear, the combination of slow growth rates, larger body size and delayed maturity are known to play an important role in the extended life span of polar marine invertebrates (Pörtner et al. 2007). The longevity of dominant polar species becomes especially relevant for estimating recovery time of an ecosystem after disturbance. According to these results, the recovery time after disturbance for Arctic shelves would be in the order of decades.

Individual production and turn-over rates

With broadcast-spawning species such as *O. sarsii* and *O. sericeum* the expectation is to have a population formed by many small sized individuals and a gradual decrease in numbers of larger individuals (Gage 2003). In the present study, the lack of very small-sized individuals for both species may be due to the use of a trawl net used with a 4-mm codend liner. Some smaller sized individuals may still be retained with the accumulation of fine mud and silt in the trawl mesh, but not quantitatively sampled. This is especially true for regions heavily influenced by riverine input, such as the central Beaufort shelf, where *O. sericeum* samples were collected (Naidu 1974, Whitefield et al. 2015). Therefore, the absence of smaller sized individuals in the size frequency distribution (especially for *O. sarsii*) could more likely be interpreted as a methodological bias and less so as the absence of new recruits.

In populations where recruitment is either very low or very infrequent and lifespan is long, the size distribution usually would show extreme negative skewness (Ebert 1983). This is not the case for the populations of *O. sarsii* and *O. sericeum* sampled in this study. Despite the lack of smaller sizes, the size frequency distribution of the two species shows a clear positive skewness. Therefore, high recruitment can be inferred, given the longevity of the two species and their positively skewed population size structure. Another pattern observed in the size distribution of both species is the presence of larger modal peaks, spanning 5-10 mm of body size. The sizes with low frequency, that are delineating the larger modes, could represent particular periods of very low recruitment for both species. Interestingly, the sizes with the lowest frequency for both species (13-15 mm for *O. sarsii* and 10-11 mm for *O. sericeum*) correspond to individuals of approximately the same age range (13-18 years), suggesting a common environmental cause.

For the Pacific Arctic in particular, the lack of long-term and seasonal studies focused on meroplankton has limited our understanding of the supply side of benthic standing stock (Hopcroft et al. 2008). Without this information, it is difficult to relate the low or high frequencies of certain size classes in our size distributions to the periodicity of low recruitment events. High density of ophioplutei of *O. sericeum* in the Kara Sea correlated well with the high density of adults found in that region (Fetzer & Deubel 2006). However, ophiuroid larvae were not found in high densities during a three-year sampling effort in our Beaufort Sea study region (C. Smoot, pers. comm.) or in the Chukchi Sea shelf (E. Ershova, pers. comm.). In addition, there is evidence that successful recruitment in polar environments can be sporadic (Brey et al. 1995, Blicher et al. 2007). The large Antarctic brittle star, *Ophionotus victoriae*, despite showing consistent timing of reproduction among years, had large inter-annual variation in reproductive effort over three years (Grange et al. 2004). Increasing this uncertainty, a study reviewing the gonad development and larval density of *O. sericeum* off northeast Greenland found that larval production occurred at a biannual rate (Thorson 1950, Pearse 1965).

Consequently, it is possible that the sample collection performed in the Kara Sea encountered a large spawning event (Fetzer & Deubel 2006), and does not represent consistent inter-annual reproductive effort. Without long-term data series of meroplankton abundance, and gonad development in adults, it is impossible to determine the inter-annual variability in spawning and recruitment, especially if low spawning events occur many years apart. In addition to reproductive periodicity, environmental drivers of reproduction, larvae and newly settled recruit success may also be an important factor contributing to the periodic low frequency sizes. The periodicity of reproduction effort and successful recruitment events are key components for understanding the stability of these populations and energy allocation within these populations.

In support of the second hypothesis, *O. sarsii* had higher individual production values compared with *O. sericeum* individuals of the same size. For both species, organic mass increased with increasing body size following the same exponential trend, also described for other brittle star species (Packer et al. 1994, Dahm 1993, Gage 2003). However, for a given size or age class, the individual production of *O. sarsii* was nearly an order of magnitude greater than the individual production of *O. sericeum* suggesting species-specific physiological characteristics. In addition, the magnitude of this difference may be enhanced by regional differences in productivity regimes in the areas where each species was collected. Regional environmental forces can have a significant influence on benthic organism growth rates and production (Carroll et al. 2011a, Carroll et al. 2011b). *Ophiura sarsii* individuals were collected in the highly productive northeast Chukchi Sea, where net primary productivity can reach 1,500 mg C m^{-2} d^{-1} (Grebmeier et al. 2009). Conversely, *O. sericeum* were collected on the less productive central Beaufort Sea shelf and upper slope, close to the Mackenzie River, with an annual primary production estimate of up to 16 g C m^{-2} (Carmack et al. 2004). This difference in water column productivity is also reflected in the benthic community biomass. The northeast Chukchi Sea benthic hotspots can reach > 4,000 g wet wt. m^{-2} in biomass for infauna and 644 g wet wt. m^{-2} for epifauna (Ravelo et al. 2014, Grebmeier et al. 2015, Denisenko et al. 2015). In contrast, the central Beaufort shelf epibenthic community has a recorded maximum biomass of 58 g wet wt. m^{-2} (Ravelo et al. 2015). In conclusion, individual brittle star production values match the productivity regimes of the NE Chukchi Sea and central Beaufort Sea.

Our third hypothesis was supported by our results in that *O. sarsii* had a higher turnover rate than *O. sericeum*. As discussed above, environmental factors have a large influence on population abundance, biomass, growth and productivity. Both total annual production and turnover rate estimates for both species were comparable to values reported for Antarctic brittle star species and considerably lower than values reported for subpolar species (Table 2, updated from Table 5-26 in Dahm (1996)). To date, changes in growth rate and productivity for the same brittle star species along temperature and food supply gradients has not been tested. Considering the near pan-Arctic shelf distribution and locally high densities of *O. sarsii* and *O. sericeum*, these species could be used as models for assessing the influence of different environmental characteristics on benthic population dynamics.

The premise for our second and third hypotheses was that the higher energetic demand of the larger *O. sarsii* excluded this species from inhabiting the less productive central Beaufort Sea. Comparing current presence/absence distribution data with data from 1970's trawl surveys reveal a distribution shift may have occurred for these two species over the past 40 years (Frost & Lowry 1983). Surveys performed from 2011 to 2014 in the central Beaufort Sea confirmed the absence of *O. sarsii* east of 148°W; while, in the 1970's this species was found as far as 141° W (Carey et al. 1974, Frost & Lowry 1984, Ravelo et al. 2015). Long-term atmospheric data indicate that an increase in the prevalence and intensity of easterly winds in the central Beaufort shelf region has occurred over the past 40 years, causing more persistent and prolonged reversals of water flow from the Chukchi Sea entering the Beaufort Sea (Hufford 1973, von Appen & Pickart 2012, Pickart et al. 2013). Through these changes, not only is the transport of *O. sarsii* larvae from the Chukchi Sea population limited to the western Beaufort Sea, but it also favors the transport of *O. sericeum* larvae towards the west. Along with the reduction in transport of high nutrient waters from the Chukchi Sea into the Beaufort Sea shelf, an extensive intrusion of the Mackenzie inflow into the central Beaufort Sea has been observed in recent decades (Whitefield et al. 2015, Ravelo et al. in review). Furthermore, *O. sericeum* often dominates in interior shelves, such as in the Laptev and Kara Seas, characterized by riverine sources of carbon and reduced primary production (Piepenburg & Schmid 1997, Fetzer & Deubel 2006, Goñi et al. 2013). With increased freshening of the central Beaufort Sea shelf, this system may be transitioning into an environment better suited for less productive species such as *O. sericeum* and less suitable for more productive species such as *O. sarsii*. Such environmentally driven distribution shifts can have large implications for higher trophic levels and the energy flow throughout the marine system. Future studies linking environmental conditions with the survival strategies of dominant, pan-Arctic species such as *O. sarsii* and *O. sericeum,* may shed light on how different environmental conditions shape benthic communities, as well as how benthic systems may be changing under current and predicted climate scenarios.

Conclusion

The information presented through this research increases our understanding of the population dynamics of *O. sarsii* and *O. sericeum*, two of the most representative species of the Arctic shelf benthos. This study has demonstrated that the largest individuals were at least a decade older than temperate region congeners, agreeing with the knowledge that polar species have slower growth rates and live longer than temperate region species.

The growth pattern of both *O. sarsii* and *O. sericeum* showed an inflection in growth, possibly related to life history mechanisms aimed to escape predation and optimize energy allocation to reproduction. Due to large variability in the size at age of the populations of both species, clear cohorts were not distinguishable from the size frequency data. However, large modal peaks spanning 5-10 mm of body size were quite clear and may be marked by extreme recruitment years. To complete our understanding of the stability of these brittle star populations over time, information regarding the supply side of recruitment is needed.

The two species investigated in this analysis differed greatly in maximum body size, longevity and individual production values. Intrinsic physiological characteristics of each species are likely the cause of such differences. However, the difference between the two species may be enhanced by bottom up controls on growth and production specific to the region where each species was collected. In the Alaskan Arctic, *O. sarsii* dominates the Chukchi Sea and western Beaufort Sea and is not present east of 148° W where *O. sericeum* dominates the shelf system. Therefore, the marked difference in regional geographic distribution of these two generally widespread species may be a consequence of their differences in energetic requirements, where unlike *O. sericeum, O. sarsii* is not able to recruit successfully in areas of lower ecosystem productivity, higher terrigenous sedimentation and fresh water input. Further research into the influence of water masses on growth and larval distribution may shed light regarding the current geographic distribution of the two species.

Acknowledgments

The authors are grateful for the hard work and dedication of the captains and crews of the USCC Healy and RV Norseman II. Special thanks to Lauren Bell, Lorena Edenfield, Kimberly Powell, and Tanja Schollmeier from the University of Alaska Fairbanks (UAF) for help with the collection of brittle stars. This manuscript and analysis benefited from the comments from Andrew Mahoney

(UAF), Christian Zimmerman (United States Geological Survey) and Peter Winsor (UAF). Samples for this analysis were collected during the 2013 COMIDA-CAB Hanna Shoal cruise (Chukchi Sea Monitoring In Drilling Area-Chemical And Benthos) and the US-Canada trans-boundary cruise, both funded by the US Department of the Interior, Bureau of Ocean Energy Management (BOEM), under Agreement Numbers M08PC20056 and M12AC00011. A. M. Ravelo would like to thank the North Pacific Research Board for the support provided during the sample processing and data analysis of this project and also the School of Fisheries and Ocean Sciences and the Advanced Instrument Lab at UAF for provided extra funds (Robert Byrd award) and a discounted rate for the use of the SEM.

A.M. Ravelo, B. Konar, B. Bluhm and K. Iken declare they have no conflicts of interests regarding the research here presented. A.M. Ravelo, B. Konar, B. Bluhm and K. Iken equaly contributed to the collection of specimens. A.M. Ravelo processed and analyzed the data, interpreted the results and wrote the manuscript. B. Konar, B. Bluhm and K. Iken also contributed to the interpretation of results and crafting of the manuscript. This article does not contain any studies with animals with applicable existing national and/or institutional guidelines for the care and use of animals.

References

Abookire AA, Rose CS (2005) Modifications to a plumb staff beam trawl for sampling uneven, complex habitats. Fish Res 71:247–254

Abramoff MD, Magalhaes PJ, Ram SJ (2004) Image processing with ImageJ. Biophotonics Int 11:36–42

Ambrose WGJ, Clough L, Tilney P, Beer L (2001) Role of echinoderms in benthic remineralization in the Chukchi Sea. Mar Biol 139:937–949

Ambrose WGJ, Caroll ML, Greenacre M, Thorrold SR, McMahon KW. (2006) Variation in *Serripes groenlandicus* (Bivalvia) growth in a Norwegian high-Arctic fjord: Evidence for local- and large-scale climatic forcing. Glob Chang Biol 12:1595–1607. doi: 10.1111/j.1365-2486.2006.01181.x

Aronson RB (1989) Brittlestar beds: low-predation anachronisms in the British Isles. Ecology 70:856–865

Arrigo KR, Perovich DK, Pickart RS, Brown ZW, van Dijken GL, Lowry KE, Mills MM, Palmer MA, Balch WM, Bates NR, Benitez-Nelson CR, Brownlee E, Frey KE, Laney SR, Mathis J, Matsuoka A, Greg MB, Moore GWK, Reynolds RA, Sosik HM, Swift JH (2014)

Phytoplankton blooms beneath the sea ice in the Chukchi sea. Deep Sea Res Part II Top Stud Oceanogr 105:1–16. doi: 10.1016/j.dsr2.2014.03.018

Arrigo KR, van Dijken GL (2015) Continued increases in Arctic Ocean primary production. Prog Oceanogr 136:60–70. doi: 10.1016/j.pocean.2015.05.002

Bell LE, Bluhm BA, Iken K (2016) Influence of terrestrial organic matter in marine food webs of the Beaufort Sea shelf and slope. Mar Ecol Prog Ser. doi:10.3354/meps11725

Blicher ME, Rysgaard S, Sejr MK (2007) Growth and production of sea urchin *Strongylocentrotus droebachiensis* in a high-Arctic fjord, and growth along a climatic gradient (64 to 77° N). Mar Ecol Prog Ser 341:89–102. doi: 10.3354/meps341089

Bluhm BA, Piepenburg D, von Juterzenka K (1998) Distribution, standing stock, growth, mortality and production of *Strongylocentrotus pallidus* (Echinodermata: Echinoidea) in the northern Barents Sea. Polar Biol 20:325–334

Bluhm BA, Iken K, Mincks Hardy S, Sirenko BI, Holladay BA (2009) Community structure of epibenthic megafauna in the Chukchi Sea. Aquat Biol 7:269–293. doi: 10.3354/ab00198

Brey T (1991) Population dynamics of *Sterechinus antarcticus* (Echinodermata: Echinoidea) on the Weddell Sea shelf and slope, Antarctica. Antarct Sci 3:251–256.

Brey T (2001) Population dynamics in benthic invertebrates. A virtual handbook. Version 01.2. In: http://www.thomas-brey.de/science/virtualhandbook

Brey T, Clarke A (1993) Population dynamics of marine benthic invertebrates in Antarctic and subantarctic environments: are there unique adaptations? Antarct Sci 5:253–266

Brey T, Pearse J, Basch L, McClintock J, Slattery M (1995) Growth and production of *Sterechinus neumayeri* (Echinoidea: Echinodermata) in McMurdo Sound, Antarctica. Mar Biol 124:279–292. doi: 10.1007/BF00347132

Carey JAG, Ruff RE, Castillo JG, Dickinson JJ (1974) Benthic ecology of the western Beaufort Sea continental margin: Preliminary results. In: Reed JC, Sayer JE (eds) Symposium on Beaufort Sea coastal and shelf research. The Arctic Institute of North America, San Francisco, pp 665–680

Carmack EC, Macdonald RW (2002) Oceanography of the Canadian Shelf of the Beaufort Sea: a setting for marine life. Arctic 55:29–45

Carmack EC, Macdonald RW, Jasper S (2004) Phytoplankton productivity on the Canadian Shelf of the Beaufort Sea. Mar Ecol Prog Ser 277:37–50

Carroll ML, Ambrose WG, Levin BS, Locke V, William L, Henkes GA, Hop H, Renaud PE (2011a) Pan-Svalbard growth rate variability and environmental regulation in the Arctic bivalve *Serripes groenlandicus*. J Mar Syst 88:239–251. doi: 10.1016/j.jmarsys.2011.04.010

Carroll ML, Ambrose WGJ, Levin BS, Ryan SK, Ratner AR, Henkes GA, Greenacre MJ (2011b) Climatic regulation of *Clinocardium ciliatum* (bivalvia) growth in the northwestern Barents Sea. Palaeogeogr Palaeoclimatol Palaeoecol 302:10–20. doi: 10.1016/j.palaeo.2010.06.001

Clarke A (1980) A reappraisal of the concept of metabolic cold adaptation in polar marine invertebrates. Biol J Linn Soc 14:77–92. doi: 10.1111/j.1095-8312.1980.tb00099.x

Dahm C (1993) Growth, production and ecological significance of *Ophiura albida* and *O. ophiura* (Echinodermata: Ophiuroidea) in the German Bight. Mar Biol 116:431–437. doi: 10.1007/BF00350060

Dahm C (1996) Ökologie und Populationsdynamik antarktischer Ophiuroiden (Echinodermata). Berichte zur Polarforsch 194:1–289

Dahm C, Brey T (1998) Determination of growth and age of slow growing brittle stars (Echinodermata: Ophiuroidea) from natural growth bands. J Mar Biol Ass UK 78:941–952

Denisenko S, Grebmeier J, Cooper L (2015) Assessing bioresources and standing stock of zoobenthos (key species, higher taxa, trophic groups) in the Chukchi Sea. Oceanography 28:146–157. doi: 10.5670/oceanog.2015.63

Divine LM, Bluhm BA, Mueter FJ, Iken K (2015) Diet analysis of Alaska Arctic snow crabs (*Chionoecetes opilio*) using stomach contents and $\delta^{13}C$ and $\delta^{15}N$ stable isotopes. Deep Res Part II Top Stud Oceanogr 1–13. doi: 10.1016/j.dsr2.2015.11.009

Dolbeth M, Cusson M, Sousa R, Pardal MA (2012) Secondary production as a tool for better understanding of aquatic ecosystems Can J Fish Aquat Sci 69: 1230–1253. doi:10.1139/F2012-050

Ebert TA (1983) Recruitent in echinoderms. In: Jangoux M, Lawrence JM (eds) Echinoderm studies. A. A. Palkema, Rotterdam, pp 169–203

Fetzer I, Deubel H (2006) Effect of river run-off on the distribution of marine invertebrate larvae in the southern Kara Sea (Russian Arctic). J Mar Syst 60:98–114. doi: 10.1016/j.jmarsys.2005.11.005

Frost KJ, Lowry LF (1983) Demersal fishes and invertebrates trawled in the northeastern Chukchi and western Beaufort Seas 1976-1977. U.S Department of Commerce NOAA Tech Rep NMFS-SSRF-764

Frost KJ, Lowry LF (1984) Trophic relationships of vertebrate consumers in the Alaskan Beaufort Sea. In: Barnes PW, Schell DM, Reimnitz E (eds) The Alaskan Beaufort Sea: ecosystems and environments. Academic Press Inc., pp 381–401

Gage JD (1990a) Skeletal growth bands in brittle stars: microstructure and significance as age markers. J Mar Biol Ass UK 70:209–224

Gage JD (1990b) Skeletal growth markers in the deep-sea brittle stars *Ophiura ljungmani* and *Ophiomusium lymani*. Mar Biol 104:427–435.

Gage JD (2003) Growth and production of *Ophiocten gracilis* (Ophiuroidea: Echinodermata) on the Scottish continental slope. Mar Biol 143:85–97

Gage JD, Tyler PA (1982) Growth and reproduction of the deep-sea brittlestar *Ophiomusium lymani* Wyville Thomson. Oceanol Acta 5:73–83

Goñi MA, O'Connor AE, Kuzyk ZZ, Yunker MB, Gobeil C, Macdonald RW (2013) Distribution and sources of organic matter in surface sediments across the North American Arctic margin. J Geophys Res Ocean 118:1–19. doi: 10.1002/jgrc.20286

Grange LJ, Tyler PA, Peck LS, Cornelius N (2004) Long-term interannual cycles of the gametogenic ecology of the Antarctic brittle star *Ophionotus victoriae*. Mar Ecol Prog Ser 278:141–155. doi: 10.3354/meps278141

Grebmeier JM, Cooper LW, Feder HM, Sirenko BI (2006) Ecosystem dynamics of the Pacific-influenced northern Bering and Chukchi seas in the Amerasian Arctic. Prog Oceanogr 71:331–361

Grebmeier JM, Harvey HR, Stockwell DA (2009) The Western Arctic Shelf-Basin Interactions (SBI) project, volume II: An overview. Deep Res Part II Top Stud Oceanogr 56:1137–1143. doi: 10.1016/j.dsr2.2009.03.001

Grebmeier JM, Bluhm BA, Cooper LW, Danielson SL, Arrigo KR, Blanchard AL, Clarke JT, Day RH, Frey KE, Gradinger RR, Kędra M, Konar B, Kuletz KJ, Lee SH, Lovvorn JR, Norcross BL, Okkonen SR (2015) Ecosystem characteristics and processes facilitating persistent macrobenthic biomass hotspots and associated benthivory in the Pacific Arctic. Prog Oceanogr 136:92–114. doi: 10.1016/j.pocean.2015.05.006

Gunderson DR, Ellis IE (1986) Development of a plumb staff beam trawl for sampling demersal fauna. Fish Res 4:35–41

Gusev AA, Jurgens-Markina EM (2012) Growth and production of the bivalve *Macoma balthica* (Linnaeus, 1758) (Cardiida: Tellinidae) in the southeastern part of the Baltic Sea. Russ J Mar Biol 38:56–63. doi: 10.1134/S1063074012010063

Hendler G (1975) Adaptational significance of the patterns of ophiuroid development. Integr Comp Biol 15:691–715. doi: 10.1093/icb/15.3.691

Hoover CA (2013) Ecosystem model indicators for the Beaufort Sea Shelf Region of the Beaufort Sea. Can Data Rep Fish Aquat Sci 1249:vi–14

Hopcroft R, Bluhm B, Gradinger R (2008) Arctic Ocean Synthesis: Analysis of climate change impacts in the Chukchi and Beaufort Seas with strategies for future research. North Pacific Research Board, Fairbanks

Hufford GL (1973) Warm water advection in the southern Beaufort Sea August - September 1971. J Geophys Res 78:2702–2707

Hyman LH (1955) The invertebrates. 4. Echinodermata. McGraw-Hill, New York

Iken K, Bluhm B, Dunton K (2010) Benthic food-web structure under differing water mass properties in the southern Chukchi Sea. Deep Sea Res Part II Top Stud Oceanogr 57:71–85

Jakobsson M, Mayer L, Coakley B, Dowdeswell JA, Forbes S, Fridman B, Hodnesdal H, Noormets R, Pedersen R, Rebesco M, Schenke HW, Zarayskaya Y, Accettella D, Armstrong A, Anderson RM, Bienhoff P, Camerlenghi A, Church I, Edwards M, Gardner JV, Hall JK, Hell B, Hestvik O, Kristoffersen Y, Marcussen C, Mohammad R, Mosher D, Nghiem SV, Pedrosa MT, Travaglini PG, Weatherall P (2012) The International Bathymetric Chart of the Arctic Ocean (IBCAO) Version 3.0. Geophys Res Lett 39:1–6. doi: 10.1029/2012GL052219

Logerwell EA, Rand KM, Weingartner TJ (2011) Oceanographic characteristics of the habitat of benthic fish and invertebrates in the Beaufort Sea. Polar Biol 1–14

Naidu AS (1974) Sedimentation in the Beaufort Sea: a synthesis. In: Marine Geology and Oceanography of the Arctic Seas. Springer, Berlin, pp 173–190

Nikolopoulos A, Pickart RS, Fratantoni PS, Shimada K, Torres DJ, Jones EP (2009) The western Arctic boundary current at 152° W: Structure, variability, and transport. Deep Res Part II Top Stud Oceanogr 56:1164–1181. doi: 10.1016/j.dsr2.2008.10.014

O'Connor BDS, McGrath D, Keegan BF (1986) Demographic equilibrium: The case of an *Amphiura filiformis* assemblage on the west coast of Ireland. Hydrobiologia 142:151–158

Packer DB, Watling L, Langton RW (1994) The population structure of the brittle star *Ophiura sarsi* Lutken in the Gulf of Maine and its trophic relationship to American plaice (*Hippoglossoides platessoides* Fabricius). J Exp Mar Bio Ecol 179:207–222. doi: 10.1016/0022-0981(94)90115-5

Pearse JS (1965) Reproductive Periodicities in Several Contrasting populations of *Odontaster validus* Koehler, a common Antarctic Asteroid. Biol Antarct Seas II Antarct Res Ser 5:39–85

Peck LS (2016) A cold limit to adaptation in the Sea. Trends Ecol Evol 31:13–26. doi: 10.1016/j.tree.2015.09.014

Pickart RS, Schulze LM, Moore GWK, Charette MA, Arrigo KR, van Dijken G, Danielson SL (2013) Long-term trends of upwelling and impacts on primary productivity in the Alaskan Beaufort Sea. Deep Sea Res Part I Oceanogr Res Pap 79:106–121. doi: 10.1016/j.dsr.2013.05.003

Piepenburg D (2000) Arctic brittle stars (Echinodermata: Ophiuroidea). Oceanogr Mar Biol Annu Rev 38:189-256

Piepenburg D (2005) Recent research on Arctic benthos: common notions need to be revised. Polar Biol 28:733–755

Piepenburg D, Schmid MK (1997) A photographic survey of the epibenthic megafauna of the Arctic Laptev Sea shelf: Distribution, abundance, and estimates of biomass and organic carbon demand. Mar Ecol Prog Ser 147:63–75. doi: 10.3354/meps147063

Piepenburg D, Voss J, Gutt J (1997) Assemblages of sea stars (Echinodermata: Asteroidea) and brittle stars (Echinodermata: Ophiuroidea) in the Weddell Sea (Antarctica) and off Northeast Greenland (Arctic): A comparison of diversity and abundance. Polar Biol 17:305–322

Pörtner HO, Peck L, Somero G (2007) Thermal limits and adaptation in marine Antarctic ectotherms : an integrative view. Phil Trans R Soc B 2233–2258. doi: 10.1098/rstb.2006.1947

Rand KM, Logerwell EA (2010) The first demersal trawl survey of benthic fish and invertebrates in the Beaufort Sea since the late 1970s. Polar Biol 34:475–488. doi: 10.1007/s00300-010-0900-2

Ravelo AM, Konar B, Bluhm BA (2015) Spatial variability of epibenthic communities on the Alaska Beaufort Shelf. Polar Biol 38:1783–1804. doi: 10.1007/s00300-015-1741-9

Ravelo AM, Konar B, Grebmeier JM, Mahoney AR (In review) What lies beneath the ice: relating seasonal sea ice patterns with benthic shelf fauna in the Alaskan Arctic. Deep Res Part II Top Stud Oceanogr

Ravelo AM, Konar B, Trefry JH, Grebmeier JM (2014) Epibenthic community variability in the northeastern Chukchi Sea. Deep Sea Res Part II Top Stud Oceanogr 102:119–131. doi: 10.1016/j.dsr2.2013.07.017

Renaud PE, Morata N, Ambrose WGJ, Bowie JJ, Chiuchiolo A (2007) Carbon cycling by seafloor communities on the eastern Beaufort Sea shelf. J Exp Mar Bio Eco 349:248-260

Roy V, Iken K, Archambault P (2015) Regional variability of megabenthic community structure across the Canadian Arctic. Arctic 68:180–192

Sejr MK, Sand MK, Jensen KT, Petersen JK, Christensen PB, Rysgaard S (2002) Growth and production of *Hiatella arctica* (Bivalvia) in a high-Arctic fjord (Young Sound, Northeast Greenland). Mar Ecol Prog Ser 244:163–169. doi: 10.3354/meps244163

Sköld M, Rosenberg R (1996) Arm regeneration frequency in eight species of ophiuroidea (Echinodermata) from European sea areas. J Sea Res 35:353–362. doi: 10.1016/S1385-1101(96)90762-5

Sköld M, Josefson A, Loo L-O (2001) Sigmoidal growth in the brittle star *Amphiura filiformis* (Echinodermata: Ophiuroidea). Mar Biol 139:519–526. doi: 10.1007/s002270100600

Stevenson A, Mitchell JGF (2016) Evidence of nutrient partitioning in coexisting deep-sea echinoids, and seasonal dietary shifts in seasonal breeders: Perspectives from stable isotope analyses. Prog Oceanogr 141:44–59. doi: 10.1016/j.pocean.2015.12.004

Storero LP, Ocampo-Reinaldo M, González RA, Narvarte MA (2010) Growth and life span of the small octopus *Octopus tehuelchus* in San Matías Gulf (Patagonia): Three decades of study. Mar Biol 157:555–564. doi: 10.1007/s00227-009-1341-8

Thorson G (1950) Reproductive and larval ecology of marine bottom invertebrates. Biol Rev 25:1–45. doi: 10.1111/j.1469-185X.1950.tb00585.x

Tyler AV (1972) Food resource division among northern, marine, demersal fishes. J Fish Res Bd Canada 29:997–1003

Tyler PA (1977) Seasonal variation and ecology of gametogenesis in the genus *Ophiura* (Ophiuroidea: Echinodermata) from the Bristol Channel. J Exp Mar Bio Ecol 30:185–197. doi: 10.1016/0022-0981(77)90011-9

von Appen W-J, Pickart RS (2012) Two configurations of the Western Arctic Shelfbreak Current in summer. J Phys Oceanogr 42:329–351. doi: 10.1175/JPO-D-11-026.1

Whitefield J, Winsor P, McClelland J, Menemenlis D (2015) A new river discharge and river temperature climatology data set for the pan-Arctic region. Ocean Model 1–15

Whitehouse GA, Aydin K, Essington TE, Hunt Jr GL (2014) A trophic mass balance model of the eastern Chukchi Sea with comparisons to other high-latitude systems. Polar Biol 37:911-939

Wilding TA, Gage JD (1995) Skeletal growth markers in the brittle star Ophiura ophiura: Do they reflect a seasonal growth pattern. In: Emson R, Smith A, Campbell A (eds) Echinoderm Research. CRC Press, Balkema, Rotterdam, pp 283–291

Woodgate RA, Weingartner T, Lindsay R (2010) The 2007 Bering Strait oceanic heat flux and anomalous Arctic sea-ice retreat. Geophys Res Lett 37:L01602. doi: 10.1029/2009GL0416

Appendix

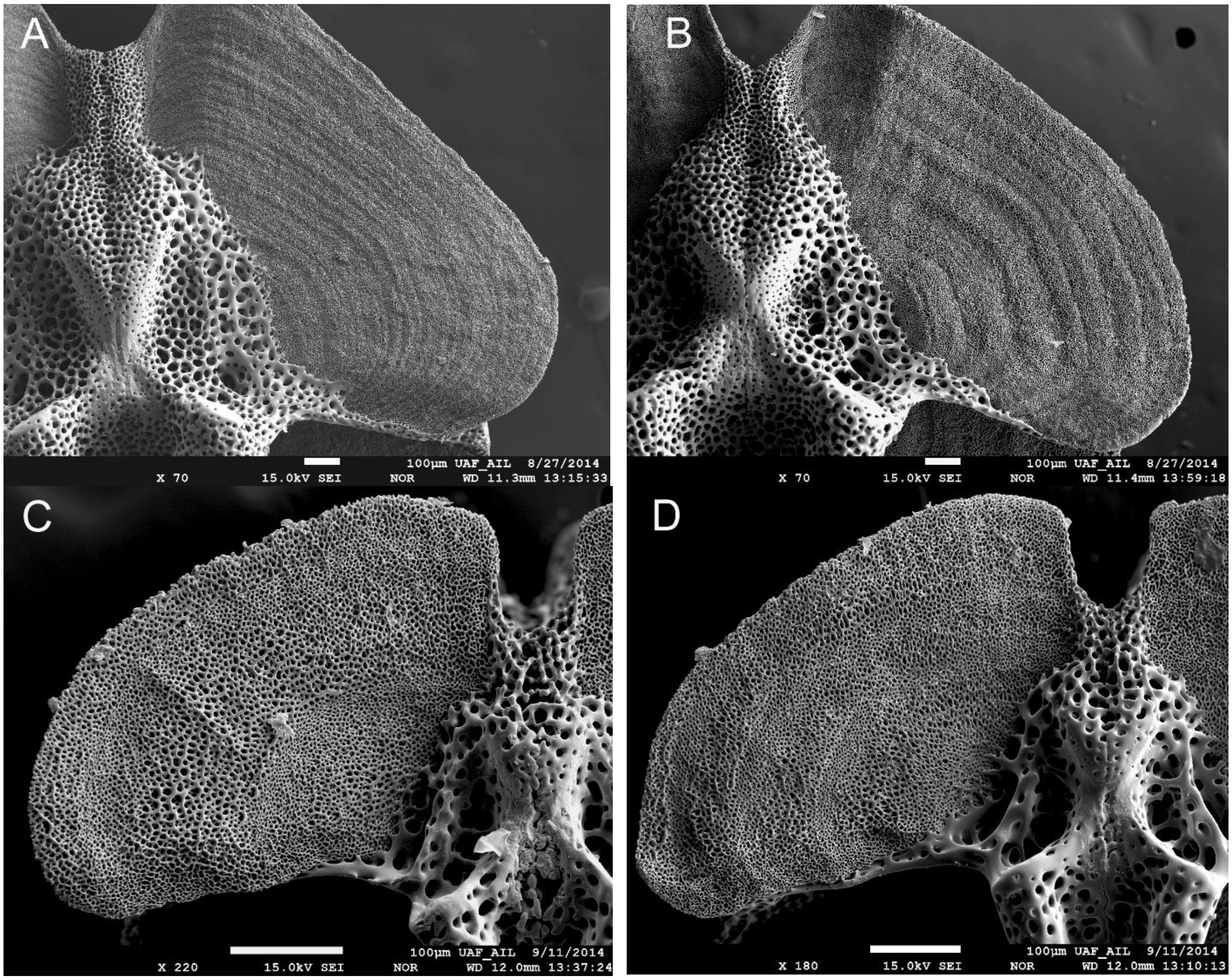

Fig. 9. Scanning electron microscope images of fossae illustrating the large intrasepecific variability in growth.*Ophiura sarsii* indivisuals of approximately the same body size and largely different age, (a) 23 years old (after correction) at 18.18 mm disc diameter and (b) 13 years old (after correction) at 18.04 mm disc diameter. *Ophiocten sericeum* individuals of approximately the same body size and largely different age, (c) 5 years old (after correction) at 8.53 mm disc diameter and (d) 8 years old (after correction) at 8.79 mm disc diamer